J. Sound Vib. (1965) **2** (2), 132–146

VIBRATIONS AND NOISE DUE TO PISTON-SLAP IN RECIPROCATING MACHINERY

ERIC E. UNGAR† AND DONALD ROSS‡

Bolt Beranek and Newman Incorporated, 50 Moulton Street, Cambridge, Mass. 02138, U.S.A.

(*Received 21 September 1964*)

A method for estimating the vibration and noise power produced by repetitive impacts in machines is presented. The dynamics of lateral piston motions across the cylinder clearance spaces of reciprocating machines are analyzed. The results of this analysis are then applied to derive estimates for the noise and vibration produced by piston-slap impacts. On the basis of some rough approximations for typical engine parameters the piston-slap-induced noise and vibrations of modern diesels are estimated.

1. INTRODUCTION

Reciprocating machinery has long been recognized to be a source of rather high levels of noise and vibration. Much work has been done in the field of machinery dynamics with the aim of reducing the essentially rigid-body, and primarily low-frequency, machine frame vibrations produced by the actions of the various inertia forces. Also, intake and exhaust silencers have been developed that can reduce the noise levels produced by intake and exhaust flows to almost any desired level (subject, of course, to the usual economic, space, and weight limitations). On the other hand, relatively little work appears to have been done on the higher frequency vibrations which involve elastic deformations of the machinery structures, and on the attendant radiated "mechanical noise". The present paper is intended as a step toward a better understanding of the mechanical noise and high frequency vibrations of reciprocating machinery.

"Mechanical noise" may be defined as that noise of a machine which remains when intake and exhaust noises are effectively absent (e.g. due to use of appropriate mufflers, or with intake and exhaust terminations located far from the machine). One may visualize many possible mechanisms that may contribute to vibrations of a machine structure, and thus to mechanical noise. These mechanisms include pressure pulses, mechanical impacts, and turbulent flows in the machine interior, as well as others associated with "accessories", such as valves, tappets, and fuel injectors. Since the types and designs of accessories may be expected to vary widely from machine to machine, there is little hope of treating the vibration and noise that these components produce with any degree of generality. Although these accessories may dominate the noise and vibration spectra of some reciprocating machines in at least some frequency ranges, there exists evidence that either "combustion noise" or "piston-slap" predominate in most cases (1, 2). The former is defined as noise directly due to pressure pulses in the cylinders, the latter as noise due to lateral impacts of pistons against the cylinder walls.

Piston-slap undoubtedly is the predominant one of these two sources of mechanical noise in machinery such as compressors, in which no high pressures or rapid pressure

† Senior Engineering Scientist, Bolt Beranek and Newman Inc., Cambridge, Mass., U.S.A.

‡ Currently on leave of absence. Present address: U.S. Navy, Office of Naval Research, London.

rises occur. It also appears that piston-slap is likely to predominate in large low-speed diesels; however, in small high-speed internal combustion engines combustion noise may take on primary importance (2).

An approach for estimating the noise and vibration levels generated by repetitive impacts is described in the first of the following sections. The mechanics of piston-slap is discussed in the second section, and the results of the first two sections are combined in the third to arrive at means for estimating the piston-slap-induced vibration and noise levels for typical machines. The latter means are combined with rough engine parameter estimates in the fourth section to illustrate their application to typical diesels.

2. VIBRATION AND NOISE PRODUCED BY IMPACTS

The striking of one machine component by another results in vibrations, which in turn result in the radiation of noise. Precise descriptions of these vibrations and of the resultant noise can be formulated only on the basis of detailed analyses, based on rather complete information on the construction, dimensions, and mechanical properties of all parts involved. However, usually relatively coarse estimates are sufficient, and such estimates may be obtained on the basis of only rather gross information about the colliding parts.

A method for estimating noise and vibration levels produced by repetitive impacts is discussed in the present section. This method, based on one commonly used in architectural acoustics (5), is applicable to a wide class of impact phenomena, although its presentation in the following paragraphs is couched in terms most directly applicable to the subsequently treated piston-slap problem.

2.1. CHARACTERIZATION OF IMPACTS

The motion induced in an elastic structure (such as a cylinder wall) by a mass (e.g. a piston) striking it is dependent on the force-velocity or mechanical impedance characteristics of the impacted structure. If one is concerned only with estimating the total vibratory energy absorbed by the latter structure, one may assume this structure to exert a retarding force proportional to, and in phase with, its local velocity. This assumption, which likens the action of the impacted structure to that of an ideal viscous dashpot [whose driving point impedance is a real rather than a complex quantity, in terms of the usual complex notation conventions (3)], may be justified on two counts:

(i) The (frequency-wise) average input impedances of finite elastic systems have been demonstrated to approach the impedances of similar infinite systems at frequencies considerably above their fundamentals (4), and the impedances of infinite plates and shells are known to be real (5). Most practical structural elements, and particularly cylinder walls or cylinder liners, fall into the plate or shell category.

(ii) For impact processes that are completed before the stress waves initiated at the first instant of contact are reflected back to the point of impact, the assumption of a real input impedance has been shown to be reasonable (5). Thus, the assumption of real impedance is justified for impacts that are relatively sharp and for impacted structures in which the return of reflections is impeded by the presence of damping or scattering.

If Z denotes the (real) input impedance of a structure which is struck by a mass M_P with velocity V_0, then one finds that after the impact the mass and the impact point on the structure move together with a velocity v which obeys

$$v = V_0 e^{-t/\tau}, \quad \tau = M_P/Z, \tag{1}$$

where t denotes time measured from the instant of contact. For an impact against a cylinder wall one may take M_P to represent the piston mass, V_0 to represent the velocity (normal

to the cylinder wall) with which the piston strikes the cylinder wall, and Z to represent the impedance of that wall.

2.2. VIBRATION SPECTRUM

By Fourier transformation of equation (1) one may find the spectrum of the pulse described by that expression. The velocity spectrum one obtains may be expressed as

$$|V(\omega_v)| = (V_0\tau/\pi)[1+(\omega_v\tau)^2]^{-1/2}, \tag{2}$$

within a multiplicative constant (that depends on the definition of the Fourier transformation one chooses, and which is of little interest here). The symbol ω_v denotes the circular (radian) vibration frequency.

One may observe that equation (2) implies a vibration velocity spectrum that is flat at low frequencies ($\omega_v\tau \ll 1$) and varies inversely with frequency at high frequencies (i.e. decreases at 6 dB per octave for $\omega_v\tau \gg 1$). Although vibration velocity spectra measured on actual machines may be expected to show the effects of resonances, anti-resonances, and attenuation of structures between the points of impact and measurement, one may reasonably anticipate that the gross character of the measured vibration over a wide frequency range will be of the nature described by this spectrum.

2.3. VIBRATORY POWER

The energy W absorbed by the impacted structure due to the one impact described by equation (1) is found to be

$$W = \int_0^\infty Fv\,dt = Z\int_0^\infty v^2\,dt = \tfrac{1}{2}M_P V_0^2. \tag{3}$$

Here F denotes the force acting on the structure, and use was made of the usual definition of impedance as $Z = F/v$.

The right-hand side of equation (3) is seen to represent the kinetic energy of the impacting mass at the instant of contact. It is thus evident that the previous assumption concerning the character of the impedance of the impacted structure amounts in essence to prescribing that this structure absorb all of the kinetic energy of the impacting mass—that is, that no energy go into rebound of the mass. Equation (3) therefore provides one in all cases with an upper bound to the vibratory energy induced in the impacted structure.

If several different impacts occur during a given cycle of operation of a reciprocating machine, then the total vibratory energy supplied by these impacts may be obtained by adding the various contributions of the individual impacts. The (time-wise) average vibratory power P_v may then be expressed as

$$P_v = \frac{1}{T_c}\sum_{\text{cycle}} W = \frac{2n}{spc}\sum_{\text{cycle}} W = \frac{nM_P}{spc}\sum_{\text{cycle}} V_0^2. \tag{4}$$

Here T_c denotes the time required for the completion of one cycle, n the rotational speed of the machine (in revolutions per unit time) and spc the number of strokes (or half-revolutions) per cycle. The summations of equation (4) are taken over all impacts that occur during a cycle; the right-hand expression is based on the premise that the same mass is involved in all these impacts, whereas the earlier expressions do not include this restriction.

2.4. SOUND RADIATION

The sound power P_a radiated from the vibrating surfaces of a machine may be written as

$$P_a = \sigma\rho_a c_a A_r v_r^2, \tag{5}$$

where ρ_a and c_a denote the density of air and the sound velocity in air (so that the product $\rho_a c_a$ represents the characteristic acoustic impedance of air). A_r and v_r^2 denote the total area and the mean square velocity of the radiating surfaces, respectively. The symbol σ represents a "radiation efficiency", which serves to compare the power radiated by the structure under consideration to that of an ideal radiator. In order to obtain useful information from equation (5) one must, of course, be able to estimate the various quantities that appear on its right-hand side.

One may obtain an estimate of the mean square velocity v_r^2 of the radiating surfaces by assuming that their average kinetic energy is equal to that of the impacted structures.† If the impacted structures have a mass M_i and vibrate with a mean square velocity v_i^2, then one may express the aforementioned energy equality as

$$M_i v_i^2 = \rho_r h_r A_r v_r^2, \tag{6}$$

where ρ_r and h_r represent the density and average thickness of the radiating structures, respectively.

The velocity v_i of the impacted structure depends on its input impedance Z and on the vibratory power P_v it receives, since $v_i^2 = P_v/Z$, and so one finds from equations (5) and (6) that one may express the ratio of acoustic to vibratory power as

$$\eta_{a/v} \equiv \frac{P_a}{P_v} = \sigma \frac{\rho_a c_a M_i}{\rho_r h_r Z} \approx \frac{\sigma}{2{\cdot}3} \left(\frac{\rho_a c_a}{\rho_r c_{Li}}\right) \left(\frac{A_i}{h_r h_i}\right). \tag{7}$$

The above approximate expression is useful for estimation purposes. It is obtained by considering the impacted structure as a plate of thickness h_i and area A_i of a material having a density ρ_i and longitudinal wave velocity c_{Li}; such a plate has a mass $M_i = \rho_i h_i A_i$ and an impedance (5)

$$Z \approx 2{\cdot}3 \rho_i c_{Li} h_i^2. \tag{8}$$

If both the impacted and the radiating surfaces are of metal, then the longitudinal wave velocities in them may be expected to be nearly equal (14). Then the term in the first pair of brackets in the approximate expression of equation (7) essentially represents the ratio between the characteristic impedance of air and that of the radiating metal.

The radiation efficiency of a structure is a measure of how well structural vibrations can excite acoustic vibrations in the surrounding medium. This parameter has been studied extensively for simple configurations, so that reasonable estimates of it may be obtained for practical structures, e.g. by treating a typical engine block side as a beam-reinforced plate (8). One usually finds that σ is between 0·01 and 0·1 for frequencies that are low enough for the wavelength associated with structural vibrations to be much smaller than the wavelengths of sound at these frequencies, and that σ approaches unity for high frequencies (where the structural vibration wavelengths are greater than the acoustic wavelengths).

3. PISTON-SLAP MECHANICS

The existence of piston-slap, i.e. of impacts associated with the sidewise motions of pistons across the cylinder clearance spaces, has long been known. However, its great potential importance in relation to the mechanical noise and vibrations of reciprocating machines appears to have been appreciated only relatively recently.

† This assumption is the most reasonable one that one can make in absence of better information. In the light of the recently developed statistical energy method for vibration analysis (6, 7), this assumption implies that the impacted and the radiating structural components are well coupled and are characterized by the same modal density (number of resonances per unit frequency interval).

Zinchenko (9, 10) seems to have been the first to emphasize the significance of piston-slap in relation to the mechanical noise of engines. He also derived expressions for the impulse associated with piston-slap, but seems to have taken inadequate account of connecting-rod inertia effects.† These effects and other complicating factors were analysed more completely by Crane (12), who solved the resulting relations by means of a computer in order to obtain some specific answers of particular interest to him. Crane left his equations in general form for his calculations; he did not introduce approximations that would have provided a clearer more general insight into piston-slap phenomena. The present section presents an analysis which to some extent parallels those of Zinchenko and of Crane, but which attempts to overcome the aforementioned shortcomings of both and presents a more extensive description of piston-slap characteristics.

3.1. PRIMARY MOTIONS AND INERTIA FORCES OF MACHINE COMPONENTS

The forces acting within a machine may most readily be studied with the aid of a diagram like Figure 1. The top part of this figure describes the geometry of a typical crank-connecting-rod-piston assembly, defines the sign conventions used here, and serves as a

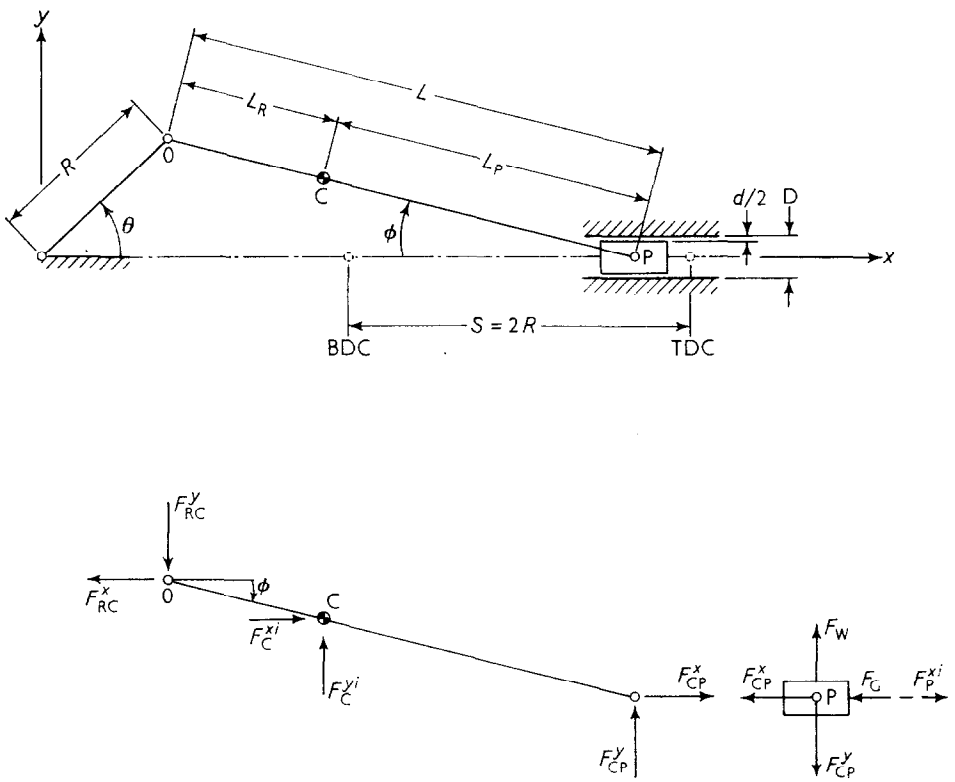

Figure 1. Piston and connecting-rod geometry and forces.

basis for the determination of the motions and inertia forces of the various machine components. These forces and the pertinent interaction forces are indicated in the "free body" diagrams of the connecting-rod and piston which appear in the lower portion of the figure.

† Zinchenko accounted for connecting-rod inertia by adding a portion of the connecting-rod mass to the piston mass. While such a procedure is known to introduce no error in the usual shaking force analyses (11), it is not *a priori* appropriate for dealing with forces within a machine.

If one takes the piston as a first approximation to be constrained to move only along its ideal kinematic axis of motion, then one may readily calculate the coordinates of the piston P and of the connecting-rod center-of-gravity C in terms of the angles θ and ϕ and the various parameters that describe the geometry of the machine (see Figure 1). The corresponding acceleration components may then be obtained by double differentiation with respect to time, taking the rotational speed $\omega = \dot{\theta}$ to be constant within the presently considered degree of accuracy. The various inertia force components then are obtained, of course, as the negatives of the products of these acceleration components and the appropriate masses.

The angle ϕ is related to the crank-angle θ as defined in Figure 1 by

$$\sin\phi = \gamma \sin\theta, \quad \gamma \equiv R/L. \tag{9}$$

The connecting-rod length L is considerably greater than the crank radius in most practical machines. Thus, $\gamma^2 \ll 1$ usually, and one may use the following approximations for the various functions of ϕ one encounters later in this analysis:

$$\begin{aligned} \cos\phi &\approx 1-(\gamma^2/2)\sin^2\theta, \\ \tan\phi &\approx \gamma\sin\theta[1+(\gamma^2/2)\sin^2\theta], \\ \phi &\approx \gamma\sin\theta+\tfrac{1}{6}(\gamma\sin\theta)^3, \\ \ddot{\phi} &\approx -\gamma\omega^2\cos\phi\sin\theta(1-\gamma^2\cos 2\theta). \end{aligned} \tag{10}$$

The various inertia force components are indicated in Figure 1. The convention that is used there is that the superscripts denote coordinate directions, with the added "i" differentiating inertia forces from forces that the components exert on each other. With the foregoing approximations one finds that one may express the inertia forces as

$$\begin{aligned} F_P^{xi} &= -M_P\ddot{x}_P = \omega^2 M_P R(\cos\theta+\gamma\cos 2\theta), \\ F_C^{xi} &= -M_C\ddot{x}_C = \omega^2 M_C(R\cos\theta+L_R\gamma^2\cos 2\theta), \\ F_C^{yi} &= -M_C\ddot{y}_C = \omega^2 M_C L_P\gamma\sin\theta. \end{aligned} \tag{11}$$

3.2. SIDE-THRUST ACTING ON PISTON

One may readily set down the equations of dynamic equilibrium for the piston in the x direction and for rotation of the connecting-rod about the pin O. From these two equations one may solve for the side-thrust force F_{CP}^y that the connecting-rod exerts on the piston. The result may be expressed as

$$\psi_S \equiv \frac{F_{CP}^y}{M_P R\omega^2\gamma} = [\psi_G-(\psi_P+\psi_C)]\sin\theta, \tag{12}$$

where

$$\begin{aligned} \psi_G &\equiv \frac{F_G\tan\phi}{M_P R\omega^2\gamma\sin\theta} \approx \frac{F_G}{M_P R\omega^2}, \\ \psi_P &\equiv \frac{F_P^{xi}\tan\phi}{M_P R\omega^2\gamma\sin\theta} \approx \cos\theta+\gamma\cos 2\theta, \\ \psi_C &\equiv \frac{(F_C^{yi}+F_C^{xi}\tan\phi)L_R\cos\phi+(r^2+L_R^2)\ddot{\phi}M_C}{L\cos\phi\cdot M_P R\omega^2\gamma\sin\theta} \approx \mu l(\nu+\cos\theta), \end{aligned} \tag{13}$$

in which r denotes the radius of gyration of the connecting-rod about an axis through its centre of gravity (and parallel to the crankshaft), and

$$\mu \equiv M_C/M_P, \quad l \equiv L_R/L, \quad \rho \equiv r/L, \quad \nu \equiv (l-2l^2-\rho^2)/l\gamma. \tag{14}$$

One may note that ψ_S represents a dimensionless side-thrust force parameter. Similarly, ψ_G, ψ_P, and ψ_C may be seen to represent the contributions to the value of this parameter made by the gas force, the piston inertia, and the connecting-rod inertia, respectively.

The approximate expressions appearing in equations (13) were obtained by use of the inertia force equations (11) and the small angle approximations of equations (10) which hold for the usually applicable inequality $\gamma^2 \ll 1$.

The term $M_P R\omega^2$, which has been used as a normalization factor in equations (13), may be recognized as representing the centrifugal force that the piston would exert if it were a point mass attached to the rotating crankshaft at the crank radius. Thus $\psi_G(\theta)$ is essentially the ratio of the gas force at crank angle θ to this centrifugal force, and ψ_P similarly is the ratio of the piston inertia force to this centrifugal force.

3.3. CONDITIONS FOR PISTON MOTION ACROSS CYLINDER CLEARANCE

Lateral motion of the piston across the cylinder clearance space may be expected to be initiated whenever the side-thrust force acting on the piston changes direction (as indicated by a change of the algebraic sign of F_{CP}^{y} or ψ_S).† One may therefore determine the crank positions θ_0 at which the aforementioned lateral motion is initiated by finding those values of θ for which the right-hand side of equation (12) changes sign, i.e. becomes zero.

Equation (12) thus indicates that lateral piston motion is initiated for $\sin\theta = 0$ and also for $\psi_G = \psi_P + \psi_C$. One accordingly expects piston-slap to occur at $\theta = 0$ (top dead center) and at $\theta = \pi$ (bottom dead center), where the side-thrust reverse is due to a change of direction of the connecting-rod axis, as well as at other "mid-stroke" positions at which the gas force contribution to side-thrust balances the total contribution from piston and connecting-rod inertia.

Diagrams like those of Figure 2 are useful for the visualization of the conditions for piston-slap-motion initiation. The upper portion of this figure shows the variation of the piston and connecting-rod inertia contributions to side-thrust (ψ_P and ψ_C) with crank-angle, as calculated from equations (13), sketched to scale for typical machine parameters ($\gamma = 1/4$, $\mu = 1$, $l = \rho = 1/3$). This plot is useful for constructing the $\psi_P + \psi_C$ curve shown in the lower portion of this figure. In addition, it indicates that ψ_P and ψ_C act essentially in phase and permits one to judge the magnitude of the discrepancy one introduces if one completely neglects the connecting-rod inertia contributions (as some investigators have done).

The lower portion of Figure 2 shows one curve representing $\psi_P + \psi_C$ (the total inertia contribution to side-thrust), together with several curves that represent different gas force contributions ψ_G. One may note that one may obtain ψ_G curves for a given machine simply by scaling of a conventional indicator diagram in accordance with the definition of ψ_G given in equations (13). Lower ψ_G curves (higher subscript numbers in Figure 2) correspond to greater operating speeds.‡

In view of equation (12), piston-slap initiation occurs for a given ψ_G curve (or operating speed for a given machine) whenever this curve intersects the $\psi_P + \psi_C$ curve. It is of interest to note that not only the shape, but also the magnitude of a ψ_G curve determines the number of possible "mid-stroke" piston-slap impacts per revolution. For example, with ψ_{G1} one obtains zero, with ψ_{G2} two, with ψ_{G3} and ψ_{G4} four, and with ψ_{G5} two such impacts, in addition to those at top and bottom dead center.

† The force F_W (see Figure 1) that the cylinder wall exerts on the piston balances F_{CP}^{y} for all practical purposes whenever the piston is in direct contact with the cylinder wall, and is in all likelihood negligibly small during the piston's lateral travel across the clearance space.

‡ Actual indicator diagrams tend to be affected but little by operating speed (13). The ψ_G curves shown in Figure 2 correspond to indicator diagrams of typical diesel engines (13), and essentially represent operation of such a diesel at several rotational speeds.

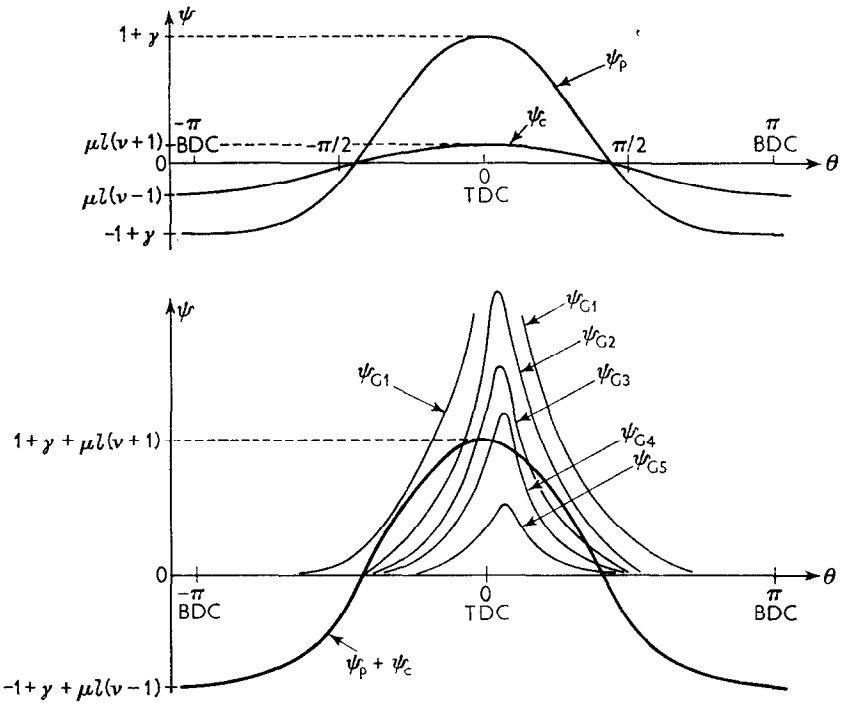

Figure 2. Inertia and gas force contributions to side thrust.

3.4. DYNAMICS OF PISTON MOTION ACROSS CLEARANCE

Since practical clearance dimensions are usually very small, one may expect pistons to traverse their clearance spaces within rather short time intervals, which are associated with only very small crank-angle increments. The side-thrust force acting on the piston during its travel across the clearance space may thus be approximated by

$$F^{y}_{CP}(\theta_0+\beta) \approx \beta[\mathrm{d}F^{y}_{CP}(\theta_0)/\mathrm{d}\theta], \tag{15}$$

where β is a small angle measured from the crank position θ_0 at which the side-thrust force changes sign and lateral piston motion is initiated.

From equations (12) and (13) one may determine that

$$\psi'_S(\theta_0) \approx [c\psi_G(\theta_0)+s\psi'_G(\theta_0)]-[2c^2-1+\gamma c(6c^2-5)]-\mu l[\nu c+2c^2-1],$$
$$c \equiv \cos\theta_0, \quad s \equiv \sin\theta_0, \tag{16}$$

where the prime denotes differentiation with respect to θ. The first bracketed term represents the contribution of the gas forces, the second that of the piston inertia, and the third that of the connecting-rod inertia forces. Thus, for top and bottom dead center piston-slaps, where $\theta_0 = 0$ and π, respectively,

$$\psi'_S(0) \approx \psi_G(0)-(1+\gamma)-\mu l(1+\nu),$$
$$\psi'_S(\pi) \approx -\psi_G(\pi)-(1-\gamma)-\mu l(1-\nu). \tag{17}$$

For "mid-stroke" piston-slaps, on the other hand, the condition $\psi_G = \psi_P+\psi_C$ combined with equation (16) yields

$$\psi'_S(\theta_0) \approx s[\psi'_G(\theta_0)+s(1+\mu l+4\gamma c)]. \tag{18}$$

The equation of motion for the piston across the clearance space (at angles θ slightly greater than θ_0) may be written as

$$F^y_{CP}(\theta_0+\beta) = \beta M_P R\omega^2 \gamma \psi'_S(\theta_0) = M_P \ddot{y} = M_P \omega^2 (d^2 y/d\beta^2), \tag{19}$$

if all forces other than side-thrust (e.g. gravity, friction as perhaps due to rings or oil films) are neglected, and if one uses equation (15) and the definition of ψ_S given in equation (12). By integration of this differential equation [i.e. the equality of the second and fourth expressions of equation (19)] one may establish that the crank rotation $\Delta\theta$ during which the piston moves across the lateral clearance distance d is given by

$$\Delta\theta = \left[\frac{6}{\gamma \psi'_S(\theta_0)}\left(\frac{d}{R}\right)\right]^{1/3}, \tag{20}$$

and that the velocity $V_0 = \dot{y}$ with which the piston contacts the opposite cylinder surface is given by

$$V_0/R\omega = \tfrac{1}{2}(\Delta\theta)^2 \gamma \psi'_S(\theta_0) = \left[\frac{9}{2}\left(\frac{d}{R}\right)^2 \gamma \psi'_S(\theta_0)\right]^{1/3}. \tag{21}$$

The quantity $R\omega$ may be recognized as the tangential velocity of a point at the crank radius R; equation (21) thus describes the ratio of the piston-slap impact velocity to this tangential velocity.

4. ESTIMATION OF VIBRATION AND NOISE DUE TO PISTON-SLAP

In order to arrive at parameters whose values can be estimated relatively readily it is convenient to refer the various power quantities to be calculated to the mechanical power P_m of the reciprocating machine being considered. In view of the definition of the mean effective pressure *mep* as the ratio of the mechanical work done (by or on the machine) to the volume swept by the piston (i.e. the piston displacement), one may express the mechanical power P_m per cylinder as

$$P_m = 2ASn(mep/spc), \tag{22}$$

where $S = 2R$ denotes the stroke (see Figure 1), A the cylinder cross-section area, and $n = \omega/2\pi$ the rotational speed in revolutions per unit time. As before, *spc* here denotes the number of strokes per cycle.

4.1. RATIO OF VIBRATORY TO MECHANICAL POWER

If one assigns the symbol $\eta_{v/m}$ to the ratio of the piston-slap induced vibratory power to the mechanical power, so that $\eta_{v/m}$ in effect represents an "efficiency" of power conversion, one may use equations (4) and (22) to obtain

$$\eta_{v/m} \equiv \frac{P_v}{P_m} = \frac{M_P}{2AS \cdot mep} \sum_{\text{cycle}} V_0^2. \tag{23}$$

Here the summation is taken over all piston-slaps that occur for one cylinder† during one cycle, and the V_0's represent piston-slap impact velocities calculated according to equation (21). By use of this equation one may rewrite equation (23) as

$$\eta_{v/m} \approx 1{\cdot}36\left(\frac{d}{R}\right)^{4/3} \gamma^{2/3} \frac{p(0)}{mep} \Gamma, \tag{24}$$

† One may note that for multi-cylinder machines both P_v and P_m are multiplied by the number of cylinders, so that the ratio $\eta_{v/m}$ is unchanged.

where

$$\Gamma \equiv \frac{cep}{p(0)} \sum_{\text{cycle}} [\psi'_S(\theta_0)]^{2/3}, \tag{25}$$

$$cep \equiv M_P R\omega^2/A, \tag{26}$$

and $p(0)$ denotes the cylinder pressure at top dead center at the end of a compression-stroke. The quantity *cep* defined in equation (26) represents a "centrifugal piston equivalent pressure", namely, the centrifugal force per unit cylinder area that the piston would exert if it were attached directly at the crank radius.

The form of equation (25) and the definition of Γ were chosen so that Γ incorporates all direct dependences on rotational speed, and so that the coefficient of Γ in equation (25) involves quantities that may be evaluated relatively readily, in general. From the definition of Γ and from equations (17) and (18) one may also ascertain that Γ depends only slightly on γ for most practical configurations. More is said later about estimates for the parameter Γ.

4.2. RATIO OF ACOUSTIC TO VIBRATORY AND TO MECHANICAL POWER

The ratio P_a/P_v of acoustic to vibratory power is given by equation (7). However, it must be recalled that all previously calculated powers were determined on the basis of one cylinder. Thus, the parameters describing the impacted structures must also be referred to a single cylinder. For example, A_i must be taken to refer to the area on which one cylinder impacts.

The ratio of acoustic to mechanical power may be obtained simply by combining equations (7) and (23):

$$\eta_{a/m} \equiv \frac{P_a}{P_m} = \eta_{a/v} \cdot \eta_{v/m}. \tag{27}$$

5. ESTIMATION OF PISTON-SLAP-INDUCED NOISE AND VIBRATIONS IN DIESEL ENGINES

It is of some interest to apply the foregoing results to estimates of piston-slap-induced noise and vibration in typical modern diesels. Such an application not only serves as an illustration of the estimation procedure advanced here, but it should also provide one with an idea of the noise and vibration levels one might expect due to piston-slap in actual engines. This application should also suggest design approaches for reducing these levels by revealing the degree to which the various parameters considered here affect these levels.

5.1. ESTIMATION OF IMPACT POWER PARAMETER Γ

The various values of $\psi'_S(\theta_0)$ that enter the calculation of Γ according to equation (25) may be determined from equations (17) and (18) for a given engine and operating condition. The values corresponding to top and bottom dead center may be obtained directly from equations (17), but in order to find the values of $\psi'_S(\theta_0)$ for mid-stroke piston-slaps one must first determine the angles θ_0 where the corresponding transverse piston motions are initiated.

The aforementioned mid-stroke transition angles θ_0 are readily obtained from plots like the lower portion of Figure 2. From experimentally obtained or theoretically predicted indicator diagrams one may plot curves of $\psi_G(\theta)$ for various assumed values of *cep*. The mid-stroke transition angles θ_0 then are those values of θ where the ψ_G curves intersect

the $\psi_P+\psi_C$ curves. One may then make use of equation (18), and finally calculate Γ for each value of *cep* from equation (25).

Figure 3 shows the result of a set of such calculations based on an idealized indicator diagram,† for the typical set of engine parameters indicated in the figure. Figure 3 shows two different curves; Γ_2 pertains to two-stroke and Γ_4 to four-stroke cycle engines. In

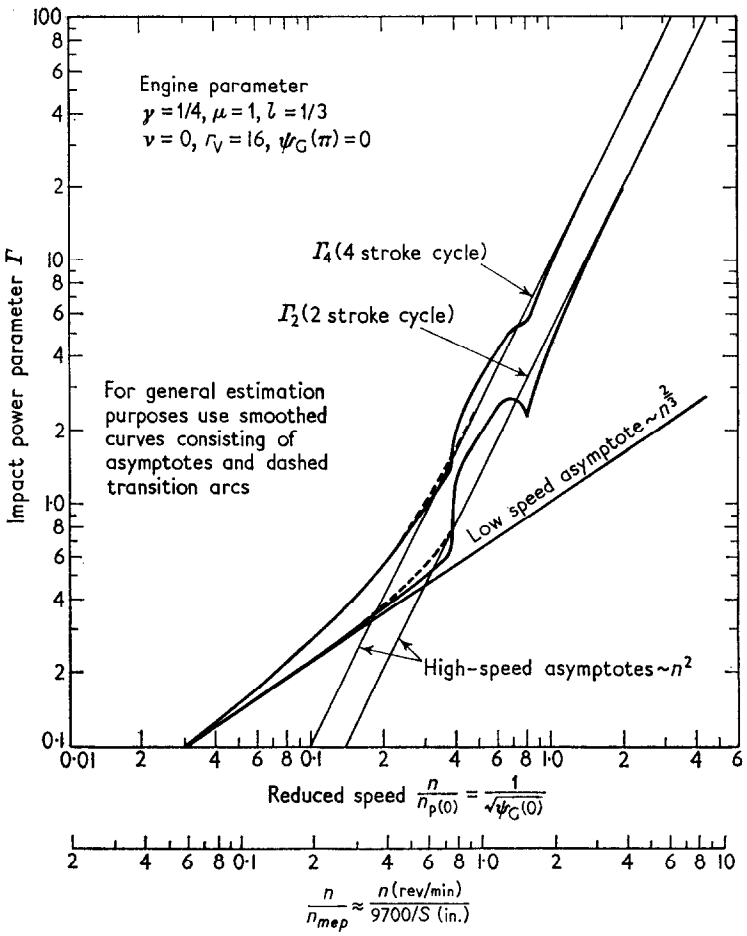

Figure 3. Speed-dependence of vibratory power induced by piston-slap.

the former a compression and expansion (power) stroke occurs during each revolution, in the latter a power stroke occurs in only every other revolution.

The parameter Γ in Figure 3 is plotted against a reduced speed parameter $n/n_{p(0)}$, where $n_{p(0)}$ is a convenient reference speed. If one chooses $n_{p(0)}$ so that

$$n/n_{p(0)} = \sqrt{cep/p(0)} = \sqrt{1/\psi_G(0)} \tag{28}$$

then $n_{p(0)}$ is that rotational speed at which $\psi_G(0) = 1$, i.e. at which the *cep* just equals the cylinder pressure at top dead center.

† Figure 3 is based on a compression process represented (15) by a pressure–volume relation with polytropic exponent 1·35 on a compression ratio taken as $r_v = 16$, and on the assumption that the expansion (power) stroke makes the same contribution to Γ as does the compression stroke; for intake and exhaust strokes ψ_G was taken as zero.

The bulges appearing in the curves of Figure 3 for reduced speeds between about 0·4 and 0·8 are associated with mid-stroke piston-slaps. Such piston-slaps are found to occur only in this speed range; for speeds outside this range the gas and inertia-contribution curves (as in the lower portion of Figure 2) do not intersect. Because the details of these curves depend to some extent on machine characteristics that are only roughly represented by the present analysis, it may be advisable to use smoothed curves, as suggested in the note on Figure 3, for general estimation.

5.2. TYPICAL DIESEL ENGINE PARAMETER VALUES

For modern diesels with compression ratios near 12 one finds that $p(0)/mep$ is of the order of 1·5 if no combustion occurs before the piston reaches the top dead center (TDC) position, or is of the order of 7 if combustion is completed approximately at TDC. Thus, one might reasonably assume an average value of $p(0)/mep \approx 3{\cdot}5$ for general estimation purposes. The ratio γ for most engines is near 1/4, and modern machines tend to be constructed with bore-to-stroke ratios near unity. With all of these values substituted into equation (24) one finds that for typical diesels

$$\eta_{v/m} \approx 4{\cdot}8(d/D)^{4/3}\Gamma, \tag{29}$$

where D denotes the engine bore (cylinder diameter).

If one lets n_{mep} represent the engine speed at which $cep = mep$ and lets s_{mep} represent the corresponding mean piston speed, then one finds from equation (26) that

$$s_{mep} = 2Sn_{mep} = \sqrt{\frac{2mep}{\pi^2}\left(\frac{AS}{M_P}\right)}. \tag{30}$$

Since the mean effective pressure mep and the piston mass per swept volume (M_P/AS) are to some extent indicative of the state of technology, one may expect the mean piston speed s_{mep} to take on essentially the same value for all modern engines. From data on a limited number of marine diesels it appears that M_P/AS for such engines is between 0·06 and 0·12 lb/in^3, with lower values applying to aluminum and higher values to cast iron pistons (1). With an average of $M_P/AS \approx 0{\cdot}09$ lb/in^3 and a value of $mep \approx 120$ lb/in^2 representative of large modern diesels (13), equation (30) leads to a value $s_{mep} \approx 1600$ ft/min. This value of mean piston speed is representative of rated operating conditions of most modern engines (13).

Since, according to equations (28) and (30),

$$n_{mep}/n_{p(0)} = \sqrt{mep/p(0)} \tag{31}$$

one may use the previous estimate of $p(0)/mep \approx 3{\cdot}5$ to construct a second reduced speed scale for Figure 3, based on n_{mep}. Such a scale is shown in the figure and has the advantage that typical rated operating conditions correspond to $n/n_{mep} = 1$ in the light of the previous discussion. From Figure 3 one thus finds that $\Gamma_2 \approx 1{\cdot}4$, $\Gamma_4 \approx 2{\cdot}8$ for rated operating conditions.

Representative data on the clearance/diameter ratio d/D are difficult to obtain. Not only are such data not usually published, but manufacturers often adjust clearances in order to suit engines to their expected service. Further, differential thermal expansion of pistons and cylinder liners tends to make clearances under running conditions differ from those measured on cold engine components. From data gathered on a very limited number of marine diesels it appears that d/D values between 10^{-3} and 5×10^{-3}, or an average $d/D \approx 3 \times 10^{-3}$, are reasonable (1).

5.3. VIBRATORY AND NOISE POWER DUE TO PISTON-SLAP

For typical marine diesels equation (29) then reduces to

$$\eta_{v/m} \approx 2 \times 10^{-3} \Gamma. \tag{32}$$

The values previously set down, $\Gamma_2 \approx 1{\cdot}4$ and $\Gamma_4 \approx 2{\cdot}8$, apply for operation at rated speed. Thus, for example, a typical 4-stroke marine diesel generating 1000 h.p. and operating at rated speed may be expected to produce about (2×10^{-3}) (2·8) (1000 h.p.) $\approx 5{\cdot}6$ h.p. of vibratory power due to piston-slap.

The ratio $(\rho_a c_a / \rho_r c_{Li})$ which appears in equation (7) turns out to be about 10^{-5} for engines with blocks (radiating surfaces) or iron or steel, or about three times that value for engines with aluminum blocks. One may estimate the area A_i on which a piston impinges to be the same as that surface of a cylinder of whose height is equal to the stroke, so that $A_i \approx \pi D^2$ since $S \approx D$. Typical cylinder wall thicknesses (16), selected so as to contain the high gas pressures generated in an engine, satisfy the relation $h_i \approx D/10$. With these estimates and taking $h_r \approx h_i$ one obtains a value of $A_i/h_r h_i \approx 300$, for the last term of equation (7).

Truly meaningful estimates of the average radiation efficiency σ for the entire audio frequency band usually of interest are difficult to obtain in general terms. However, since σ for typical engine block structures may vary between 10^{-2} and 10^{-1}, perhaps $\sigma \approx 3 \times 10^{-2}$ might represent a rough typical average value.

With all of the foregoing estimates, equation (7) leads to

$$\eta_{a/v} \approx \begin{Bmatrix} 4 \times 10^{-5} \text{ for iron or steel engine blocks} \\ 12 \times 10^{-5} \text{ for aluminum engine blocks} \end{Bmatrix}. \tag{33}$$

Thus, the 1000 hp four-cycle diesel of the previous example may be expected to generate (4×10^{-5}) (5·6 h.p.) $\approx 2 \times 10^{-4}$ h.p. $\approx 0{\cdot}2$ W of acoustic power due to piston-slap (at rated speed), if it has a cast-iron block. A similar engine with an aluminum block would be expected to produce three times as much sound power, whereas a cast-iron two-stroke engine with the same power output would produce only half as much piston-slap noise.

6. CONCLUDING REMARKS

6.1. SUMMARY AND CONCLUSIONS

A procedure has been presented by means of which one may estimate the vibration and noise power levels generated by repetitive impacts. The dynamics of piston-slap have been discussed in relation to the quantities needed for application of the foregoing estimation method. Finally, the impact and piston-slap analyses have been combined, together with some rather rough approximations to typical engine parameters, to arrive at estimates of piston-slap-induced vibration and noise levels in typical diesels.

Although one may question some of the very rough numerical results and the omission of such factors as piston rotation, the analysis nevertheless does give an indication of the importance of many of the parameters involved. One finds that one may reduce the vibrations produced by piston-slap by:

(i) reducing d/R, the ratio of clearance to crank-radius,

(ii) isolating the cylinder liner from the engine block, and possibly increasing the damping of the liner,

(iii) operating at lower speeds, for which the impact parameter Γ is lower,

(iv) reducing $p(0)/mep$, the ratio of pressure at TDC to mean effective pressure,

(v) reducing $\gamma = R/L$, the ratio of crank-radius to connecting-rod length.

Any measure that reduces the vibrations induced by piston-slap also reduces the corresponding radiated noise proportionally. In addition, one may reduce this noise, in view of equation (7) by:

(i) using thicker impacted structures, i.e. thicker cylinder walls or cylinder liners (large h_i),

(ii) using thicker radiating (i.e. engine block) structures (larger h_r) of higher-density materials (larger ρ_r), with reduced radiating areas A_i and lower radiation efficiencies σ.

6.2. DISCUSSION

Although this analysis has led to predictions of the noise and vibrations due to piston-slap, the present work makes no attempt to assess the importance of piston-slap relative to that of other potential noise and vibration sources. One may reasonably expect piston-slap to dominate the "mechanical noise" of reciprocating compressors with quiet accessories, where there is no "combustion noise". However, for reciprocating machines in general one requires experimental data in order to determine whether and under what conditions piston-slap noise predominates. A possible means for studying this dominance would consist of comparing experimentally observed dependences of noise and vibrations on various engine parameters (e.g. speed, piston mass, clearance) with dependences implied by the development presented here.

However, it must be pointed out that the present analysis is not entirely complete, and that it may fail to consider some parameters conceivably of considerable importance. The most important likely discrepancy between the present analysis and reality is associated with the tacit assumptions that were made that all forces acting on the piston act through its center of gravity, and that the wrist-pin centerline passes through this center of gravity. Thus, rotation or cocking of the piston during its travel across the clearance space has been neglected, although such rotations may have possibly marked effects on the character as well as on the severity of the piston-slap impacts.

Other shortcomings may be associated with the neglect of piston-ring friction, of oil-film-cushioning, of angular accelerations of the crankshaft, of clearances at the crankshaft bearings, and of clearances and friction torques at the wrist-pin and crank-pin. However, one may entertain the reasonable hope that these omissions are of minor importance.

ACKNOWLEDGMENT

The work presented in this paper was undertaken under the sponsorship of the U.S. Navy, Bureau of Ships, under contract NObs 88480. The authors are indebted to Lt. Franklin F. Alvarez, USN, for conducting a thorough literature survey and for checking parts of the analysis in the course of carrying out a related study.

REFERENCES

1. E. E. UNGAR, D. ROSS and F. F. ALVAREZ 1964 (January) *Bolt Beranek and Newman Inc. Report No.* 1106. Piston-slap noise in reciprocating machinery. Prepared for Dept. of the Navy, Bureau of Ships, under Contract NObs 88480.
2. D. ROSS and E. E. UNGAR 1964 (July) *Bolt Beranek and Newman Inc. Report No.* 1139. Recent experimental studies of mechanical noise in diesel engines. Prepared for Dept. of the Navy, Bureau of Ships, under Contract NObs 88480.
3. S. H. CRANDALL 1958 in *Mechanical Impedance Methods for Mechanical Vibrations*, Ed. by R. Plunkett. New York: Amer. Soc. Mech. Engrs. Section 2: Impedance and mobility analysis of lumped parameter systems.

4. E. J. SKUDRZYK 1958 *J. Acoust. Soc. Amer.* **30**, 1140. Vibrations of a system with a finite and with an infinite number of resonances.
5. L. CREMER 1953 *Acustica* **3**, 317. Calculation of sound propagation in structures.
6. R. H. LYON 1964 (February) *Shock, Vibration and Associated Environments Bulletin No.* 33, Part II, pp 13–24. An energy method for prediction of noise and vibration transmission.
7. R. H. LYON and G. MAIDANIK 1964 *AIAA Journal* **2**, 1015. Statistical methods in vibration analysis.
8. G. MAIDANIK 1962 *J. Acoust. Soc. Amer.* **34**, 809. Response of ribbed panels to reverberant acoustic fields.
9. V. I. ZINCHENKO 1956 *Vestnik Mashinostroyeniya* **4**, 13. Effect of constructional factors on the noise of ships' engines.
10. V. I. ZINCHENKO 1957 *Noise of Marine Diesel Engines*. Sudpromgiz.
11. A. R. HOLOWENKO 1955 *Dynamics of Machinery*. New York: John Wiley. See pp. 295–300.
12. P. H. G. CRANE 1959 (August) *Admiralty Research Laboratory Report ARL/R2/B10*. The initiation of diesel engine cylinder liner vibrations by piston transverse motion.
13. C. F. TAYLOR and E. S. TAYLOR 1961 *The Internal Combustion Engine*. New York: International Textbook Co., 2nd Edition. See pp. 65–76.
14. E. E. UNGAR 1964 in *Mechanical Design and Systems Handbook*, Ed. by H. A. Rothbart. New York: McGraw-Hill Book Co., Inc. Section 6: Mechanical vibrations (Table 6.10, pp. 6–71).
15. J. W. ANDERSON in *Kent's Mechanical Engineers' Handbook*, 12th Edition. New York: John Wiley. See section on "Diesel engines" in Power Volume, pp. 13–07, 13–08.
16. H. E. DEGLER 1938 *Internal Combustion Engines*. New York: John Wiley. See pp. 267–270.